Cell, Vol. 123, 75–87, October 7, 2005, Copyright ©2005 by Elsevier Inc. DOI 10.1016/j.cell.2005.07.027

Centriolin Anchoring of Exocyst and SNARE Complexes at the Midbody Is Required for Secretory-Vesicle-Mediated Abscission

Adam Gromley,[1,3] Charles Yeaman,[2] Jack Rosa,[1] Sambra Redick,[1] Chun-Ting Chen,[1] Stephanie Mirabelle,[1] Minakshi Guha,[1] James Sillibourne,[1] and Stephen J. Doxsey[1,*]
[1]Program in Molecular Medicine
University of Massachusetts Medical Center
Worcester, Massachusetts 01605
[2]Department of Anatomy and Cell Biology
University of Iowa
Iowa City, Iowa 52242

Summary

The terminal step in cytokinesis, called abscission, requires resolution of the membrane connection between two prospective daughter cells. Our previous studies demonstrated that the coiled-coil protein centriolin localized to the midbody during cytokinesis and was required for abscission. Here we show that centriolin interacts with proteins of vesicle-targeting exocyst complexes and vesicle-fusion SNARE complexes. These complexes require centriolin for localization to a unique midbody-ring structure, and disruption of either complex inhibits abscission. Exocyst disruption induces accumulation of v-SNARE-containing vesicles at the midbody ring. In control cells, these v-SNARE vesicles colocalize with a GFP-tagged secreted polypeptide. The vesicles move to the midbody ring asymmetrically from one prospective daughter cell; the GFP signal is rapidly lost, suggesting membrane fusion; and subsequently the cell cleaves at the site of vesicle delivery/fusion. We propose that centriolin anchors protein complexes required for vesicle targeting and fusion and integrates membrane-vesicle fusion with abscission.

Introduction

Cytokinesis is a fundamental process that results in division of a single cell with replicated DNA into two daughters with identical genomic composition (see (Glotzer, 2001, 2005; Guertin et al., 2002). Early events in animal cell cytokinesis include assembly and contraction of the actomyosin ring to form the cleavage furrow. Continued furrowing results in constriction of the plasma membrane to form a narrow cytoplasmic bridge between the two nascent daughter cells. Within this intercellular bridge are bundled microtubules and a multitude of proteins that together form the midbody. In a poorly understood final step called abscission, the cell cleaves at the intercellular bridge to form two daughter cells.

Membrane trafficking is required for late stages of cytokinesis (Albertson et al., 2005; Finger and White, 2002; Jurgens, 2005; Papoulas et al., 2004; Strickland and Burgess, 2004). In *C. elegans* embryos, inhibition of Golgi secretion by brefeldin A (BFA) resulted in late-stage cytokinesis defects (Skop et al., 2001). More recent studies in mammalian cells using dominant-negative approaches showed that the membrane-fusion-inducing SNARE components, syntaxin-2 and endobrevin/VAMP8, are required for a final step in cell cleavage (Low et al., 2003). Endocytic traffic also plays a role in cytokinesis. Recycling endosomes and associated components localize to the midbody and are required for cell cleavage (Monzo et al., 2005; Wilson et al., 2005; Thompson et al., 2002). However, little is known about the spatial and temporal control of dynamic membrane compartments and molecules during abscission or how these activities are coordinated to achieve cell cleavage.

The role of membrane-vesicle-tethering exocyst complexes in animal cell abscission is poorly understood. The exocyst is a multiprotein complex that targets secretory vesicles to distinct sites on the plasma membrane. In the budding yeast *S. cerevisiae*, exocyst components localize to the mother-bud neck, the site of cytokinesis (Finger et al., 1998; Mondesert et al., 1997). Exocyst disruption results in accumulation of vesicles at this site (Salminen and Novick, 1989) and impairs actomyosin-ring contraction and cell cleavage (Dobbelaere and Barral, 2004; Verplank and Li, 2005). In the fission yeast *S. pombe*, exocyst components localize to the actomyosin ring (Wang et al., 2002). Mutants for the exocyst component Sec8 accumulate 100 nm "presumptive" secretory vesicles near the division septum and cannot complete extracellular separation of the two daughter cells. A screen for cytokinesis mutants in *Drosophila melanogaster* identified the exocyst component sec5 (Echard et al., 2004), and proteomic analysis of the midbody in mammalian cells showed that the exocyst protein sec3 is at the midbody (Skop et al., 2004). Mammalian exocyst components are involved in secretion in polarized epithelial cells (Yeaman et al., 2004) and localize to the midbody (Skop et al., 2004; Wilson et al., 2005), but the function of the exocyst during cytokinesis is unclear.

Components of membrane-vesicle-tethering and -fusion complexes have been identified in some organisms and linked to cytokinesis, but the pathway that integrates these complexes with vesicle trafficking during cell cleavage is unknown. Little is known about how SNAREs and the exocyst are anchored at the midbody or how they modulate membrane-vesicle organization and fusion to coordinate abscission. Moreover, the origin and dynamics of membrane compartments involved in abscission have not been investigated. In this manuscript, we describe a multistep pathway for abscission that requires a scaffold protein to anchor

*Correspondence: stephen.doxsey@umassmed.edu
[3]Present address: Department of Genetics and Tumor Cell Biology, St. Jude Children's Research Hospital, Memphis, Tennessee, 38105.

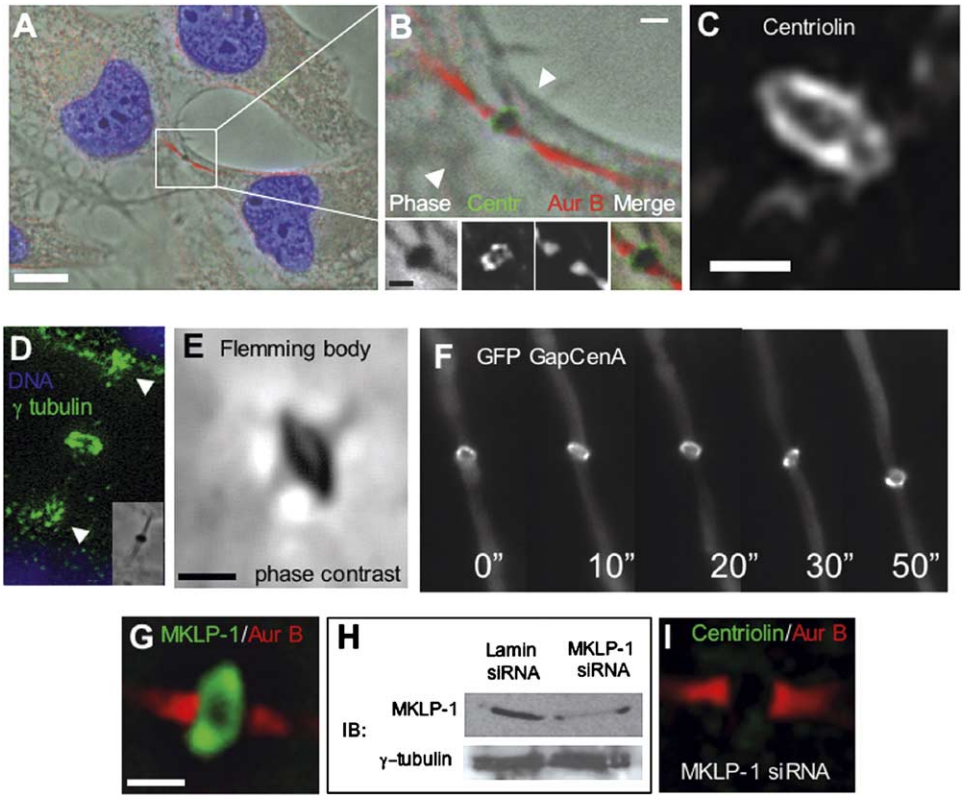

Figure 1. Centriolin Localizes to a Midbody Ring

(A) Immunofluorescence/phase image of HeLa cell during cytokinesis showing the phase-dense Flemming body within the larger diameter of the plasma membrane (arrowheads in [B]).

(B and C). Boxed region enlarged with insets (B) to show the centriolin ring (Centr, enlarged in [C]) as part of the Flemming body (phase) and flanked bilaterally by Aurora B (Aur B).

(D) γ-tubulin localizes to the midbody ring (inset, Flemming body) and sites of presumed microtubule minus ends (arrowheads).

(E) The Flemming body forms a ring.

(F) GFP-tagged GAPCenA localizes to the midbody ring and is highly dynamic (time in s).

(G–I) MKLP-1 localizes to the midbody ring (G) and, upon depletion, mislocalizes centriolin from the midbody (I). Immunoblots (IB) from cells treated with siRNAs targeting MKLP-1 or lamin A/C (control) (H). γ-tubulin, loading control. Scale bars in (A), 10 μm; (B), 5 μm; (C), (E), and (G), 1 μm.

SNARE and exocyst complexes at a unique midbody site and also requires asymmetric transport and fusion of secretory vesicles at this site.

Results

Centriolin Is Part of a Ring-like Structure at the Central Midbody during Cytokinesis

We previously showed that centriolin localized to the midbody during cytokinesis (Gromley et al., 2003). Using high-resolution deconvolution microscopy, we now demonstrate that centriolin is part of a unique ring-like structure within the central portion of the midbody, which we call the midbody ring (observed in ~75% of all telophase cells, Figures 1A–1C). The midbody ring was 1.5–2 μm in diameter (Figure 1C), contained γ-tubulin (Figure 1D), and colocalized with the phase-dense Flemming body (Figure 1B, inset) (Paweletz, 1967). In fact, high-magnification phase-contrast imaging revealed that the Flemming body was organized into a ring-like structure (Figure 1E). The midbody ring was flanked by Aurora B kinase, which colocalized with microtubules on either side of the ring (Figure 1B, inset). Several other proteins localized to the midbody ring including ectopically expressed GFP-GAPCenA, a GTPase-activating protein previously shown to localize to centrosomes (Cuif et al., 1999). Time-lapse imaging of GFP-GAPCenA and other proteins in living cells showed that the midbody ring was dynamic, moving between cells and tipping from side to side to reveal the ring structure (Figure 1F; see also Movie S1 in the Supplemental Data available with this article online). In addition, midbody-ring localization of GFP-GAPCenA confirmed the ring structure seen by immunofluorescence microscopy and demonstrated that there were no antibody penetration problems in this midbody region as seen for other antigens (Saxton and McIntosh, 1987). The midbody ring was distinct from the actomyosin ring and did not change in diameter during cytokinesis (Figures 1A and 1B). It appeared during the early stages of actomyosin-ring constriction and persisted until after cell cleavage (see below).

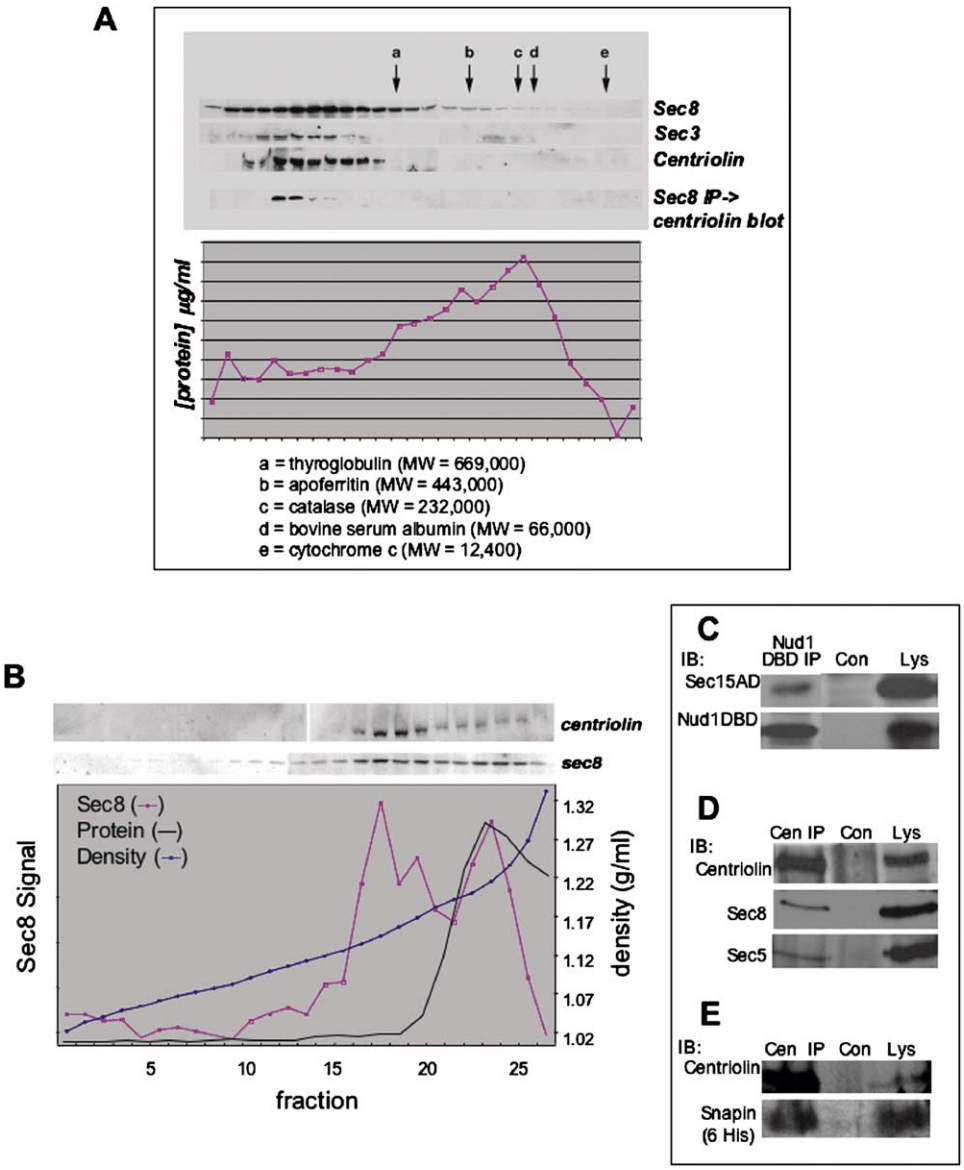

Figure 2. Centriolin Interacts with Exocyst Components and Snapin

(A) Gel filtration (Superose 6) using MDCK cell lysates shows that centriolin coelutes with peak exocyst fractions (top). Immunoprecipitation (IP) of sec8 coprecipitates centriolin. Graph, total protein profile; markers a–e are indicated.

(B) Following isopycnic centrifugation (iodixanol), centriolin comigrates in peak fractions containing sec8 (upper panels). Graph shows sec8 levels, iodixanol density, and total protein.

(C) Immunoprecipitation (IP) of Nud1-DBD (DBD antibody) pulls down sec15-AD (left). DBD, DNA binding domain; AD, activation domain; Con, control beads; Lys, lysate.

(D) Endogenous exocyst components coimmunoprecipitate with endogenous centriolin (Cen IP).

(E) Endogenous centriolin immunoprecipitates (Cen IP) overexpressed His_6-tagged snapin.

The centralspindlin components MKLP-1/CHO1/ZEN-4 (Figure 1G) and MgcRacGAP/CYK-4 (data not shown) also localized to the midbody ring and appeared earlier than centriolin during actomyosin-ring constriction. Depletion of MKLP-1 by RNAi to 18% of control levels (n = 2 experiments) prevented recruitment of centriolin to the ring (Figures 1H and 1I). In contrast, depletion of centriolin had no effect on the localization of MKLP-1 or MgcRacGAP (data not shown). These data suggested that centralspindlin anchored centriolin to the midbody ring.

Centriolin Interacts with the Exocyst Complex and the SNARE-Associated Protein Snapin and Is in Membrane-Associated Cytoplasmic Fractions

To determine the molecular function of centriolin in cytokinesis, we performed a yeast two-hybrid screen using a 120 amino acid domain of centriolin that is required for the cytokinesis function of centriolin and shares homology with budding- and fission-yeast genes (Nud1/Cdc11) involved in cytokinesis and mitotic exit (Gromley et al., 2003). A screen of approximately 12 million clones from a human testis cDNA library

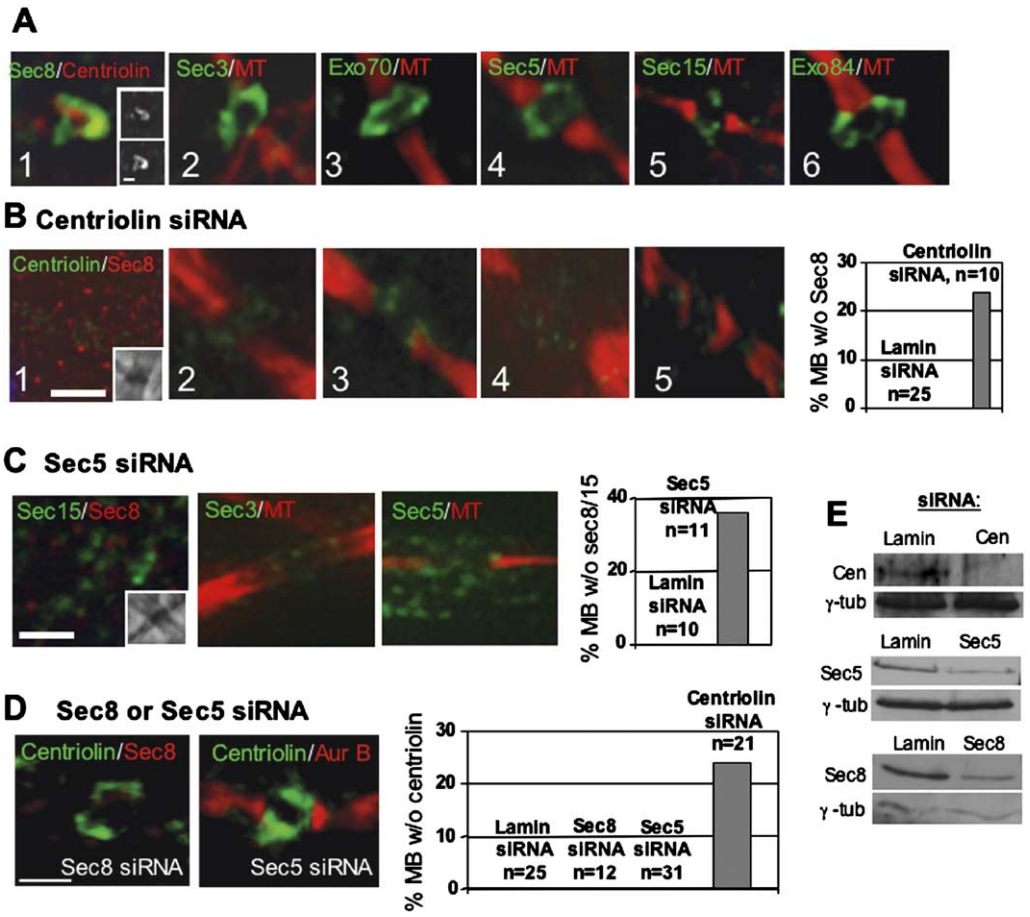

Figure 3. Exocyst Localization to the Midbody Ring Is Centriolin Dependent

(A) Immunofluorescence images of exocyst components (green) costained with centriolin antibodies (panel 1) or with anti-α-tubulin antibody (red) to visualize microtubules (MTs, panels 2–6). Panel 1 inset: top, sec8; bottom, centriolin.

(B) Cells depleted of centriolin lack midbody-associated exocyst. Images labeled as in A1–A5; B1 inset, Flemming body. Graph, percentage of midbodies (MB) without (w/o) sec8 signal following treatment with siRNAs targeting lamin A/C or centriolin; other cells have reduced levels (see text).

(C) siRNA depletion of sec5 disrupts the exocyst from midbodies costained with two exocyst proteins (C1 inset, phase) or one exocyst protein and microtubules (C2–C3). Graph, percentage of midbodies (MB) lacking sec5 staining in cells treated with lamin A/C or sec5 siRNAs.

(D) Exocyst disruption by siRNAs does not affect centriolin midbody localization. Graph, percentage of midbodies (MB) lacking centriolin stain following treatment of indicated siRNAs. Scale bar equals 1 μm (all panels).

(E) Immunoblots showing reduction of proteins targeted by siRNAs. γ-tubulin (γ-tub), loading control. Cen, centriolin.

yielded two potential interacting proteins: sec15, a member of the exocyst complex, and snapin, a SNARE-associated protein.

Additional biochemical analysis confirmed the yeast two-hybrid interactions and demonstrated that centriolin was in a large complex associated with membranes (Figure 2). The centriolin Nud1 domain fused to the DNA binding domain (DBD) and sec15 fused to the activation domain (AD) were coexpressed in the same yeast cells. Immunoprecipitation of the Nud1 fusion protein effectively coprecipitated the sec15 fusion protein (Figure 2C). To test whether other members of the exocyst complex were bound to centriolin, we immunoprecipitated endogenous centriolin from HeLa cell lysates with affinity-purified centriolin antibodies and showed that sec8 and sec5 coprecipitated (Figure 2D). Gel filtration experiments (Superose 6) using MDCK cell lysates demonstrated that centriolin coeluted with fractions containing the exocyst complex (detected with antibodies to sec8 and sec3, Figure 2A). Centriolin was eluted as a single peak that overlapped with peaks of sec3 and sec8. We next asked if centriolin coimmunoprecipitated with the exocyst. Antibodies to sec8 were added to each of the fractions from the gel filtration column, and immune complexes were collected and probed with affinity-purified centriolin antibodies as described (Gromley et al., 2003). Centriolin was found only in fractions containing exocyst components (Figure 2A). The centriolin-containing fractions eluted earlier than the peak of sec 3 or sec8, suggesting that the exocyst fraction to which centriolin was bound was different from the cytosolic and lateral plasma-membrane fractions of the exocyst (Yeaman et al., 2004). The exocyst-centriolin fractions did not cofractionate with the

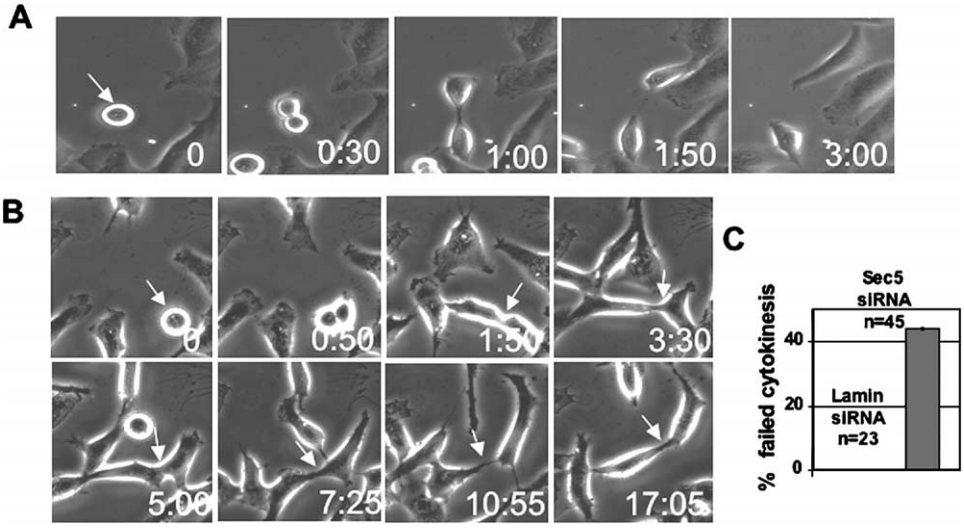

Figure 4. Exocyst Disruption Induces Cytokinesis Defects

(A) Time-lapse images of a HeLa cell treated with lamin A/C siRNAs showing a mitotic cell entering mitosis (arrow), forming a cleavage furrow, and cleaving into two separate cells in 3 hr. Time, hr:min.

(B) A cell depleted of sec5 enters mitosis (arrow), forms a cleavage furrow with normal timing (~50 min), and remains interconnected by a thin intercellular bridge for over 17 hr (panels 1:50 through 17:05).

(C) Graph shows percentage of mitotic cells that fail cytokinesis; many others are delayed (see text).

bulk of the cellular protein and eluted considerably earlier than thyroglobulin (MW 669,000) suggesting it was part of a large complex.

Since the exocyst associates with membrane vesicles, we next tested whether centriolin was also present in membranous fractions. Cell homogenates were prepared in the absence of detergent and underlain at the bottom of linear iodixanol gradients. Isopycnic centrifugation was performed, and fractions were probed for both centriolin and the exocyst component sec8. Centriolin "floated up" to fractions lighter than the cytosol having a buoyant density of $\delta \sim 1.14$ g/ml (Figure 2B). The centriolin peak cofractionated with a major peak of Sec8 that was slightly less dense than the junction-associated peak of Sec8 described previously in confluent MDCK cells ($\delta \sim 1.16$ g/ml; Yeaman et al., 2004). Little to no centriolin was observed at other positions in the gradient or in the major protein peak, suggesting that most if not all centriolin was associated with membranes. Taken together, the density gradient, immunoprecipitation, and chromatography data support the conclusion that centriolin associates with the exocyst in a very large complex bound to cellular membranes. The yeast two-hybrid interaction between centriolin and the low-abundance protein snapin was confirmed by showing that endogenous centriolin coimmunoprecipitated a His_6-tagged snapin fusion protein expressed in HeLa cells (Figure 2E) and by the centriolin-dependent midbody localization of snapin (see below).

The Exocyst Complex Colocalizes with Centriolin at the Midbody Ring

Further support for the centriolin-exocyst interaction was obtained by showing that exocyst-complex components localized to the midbody ring with centriolin. HeLa cells were colabeled with antibodies against one of several exocyst components (sec3, sec5, sec8, sec15, exo70, or exo84) and either microtubules or centriolin (Figure 3A). We found that all these exocyst components localized to the midbody ring during cytokinesis and formed a ring-like structure similar to that seen for centriolin. In fact, double-stained images revealed considerable overlap between sec8 and centriolin, indicating that they were part of the same structure (Figure 3A, panel 1). We also showed that a myc-tagged form of sec8 localized to the midbody ring when expressed in HeLa cells (Figure S1), confirming the localization seen with antibodies directed to the endogenous protein.

Midbody Localization of the Exocyst Is Disrupted in Cells Depleted of Centriolin

We next tested whether centriolin was required for midbody-ring localization of the exocyst. siRNA-mediated depletion of centriolin resulted a in ~70% reduction in centriolin protein levels and complete loss of midbody staining in 24% of cells compared with control cells treated with lamin siRNA (Figures 3B and 3E). Immunofluorescence quantification of midbody signals performed as in our previous studies (Gromley et al., 2003) demonstrated that many of the remaining centriolin-depleted cells had lower levels of midbody staining than controls (48%, n = 23 cells), bringing the total percentage of midbody depleted cells to 72%. Cells that lacked detectable midbody-associated centriolin usually lacked midbody labeling of sec8 (10/10, Figure 3B, panels 1 and 6). Although other exocyst components could not be costained with centriolin because all were detected with rabbit antibodies like centriolin, all were lost from or reduced at midbodies in centriolin-depleted cells (Figure 3B, panels 2–5). For example,

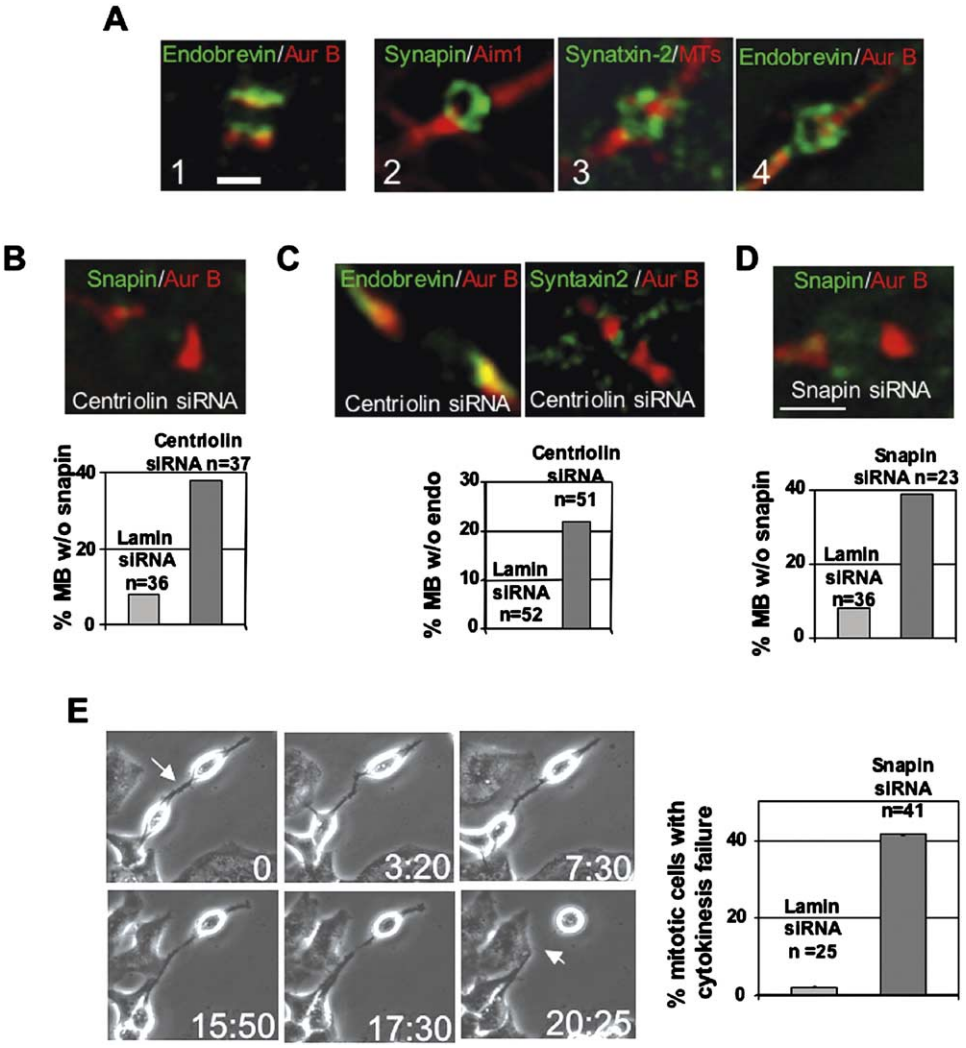

Figure 5. Centriolin siRNA Mislocalizes Midbody-Ring-Associated SNAREs and Snapin, which Disrupts Cytokinesis When Depleted

(A) Endobrevin/VAMP8 (1) localizes adjacent to the midbody ring when snapin is on the ring (2). Later, when the midbody diameter is thin (0.5–1 μm), endobrevin/VAMP8 and syntaxin-2 localize to the ring (3 and 4).

(B) Centriolin-depleted cell shows loss of snapin from the midbody ring (green). Graph, percentage of midbodies lacking snapin after siRNA depletion of proteins.

(C) Centriolin-depleted cells lose SNARE proteins from the midbody ring. Graph, percentage of midbodies lacking endobrevin/VAMP8 staining after indicated siRNAs treatments. Endo, endobrevin.

(D) Snapin-depleted cells show loss of snapin from the midbody ring. Graph, percentage of midbodies lacking snapin after indicated siRNA treatments.

(E) A snapin-depleted cell in cytokinesis (0) remains connected by a thin intercellular bridge for >17 hr before separating (20:25) (time, hr:min). Graph, percentage of mitotic cells that failed cytokinesis.

Exo84 was undetectable at midbodies in 22% of centriolin-depleted cells (n = 9 cells) or had levels below the lowest control midbody staining in 42% of centriolin-depleted cells (n = 19 cells). Significant reduction in midbody staining of centriolin and other exocyst components was observed with a second siRNA targeting a different centriolin sequence (Gromley et al., 2003) (data not shown).

To test whether centriolin was dependent on the exocyst complex for localization to the midbody, we initially targeted sec5 for siRNA depletion. Recent studies showed that mutants of sec5 in *D. melanogaster* disrupted exocyst function (Murthy and Schwarz, 2004) and that RNAi-mediated depletion of sec5 inhibited exocyst-dependent processes in vertebrate cells (Prigent et al., 2003). We found that depletion of sec5 resulted in loss of midbody-associated sec5 as well as other exocyst components, including sec3, sec8, and sec15 (Figures 3C and 3E). These results show that sec5 depletion disrupts midbody-ring localization of the exocyst. In contrast, neither sec5 nor sec8 loss from the midbody affected the association of centriolin with the midbody ring (Figures 3D and 3E). These data demonstrate that centriolin is required for midbody localiza-

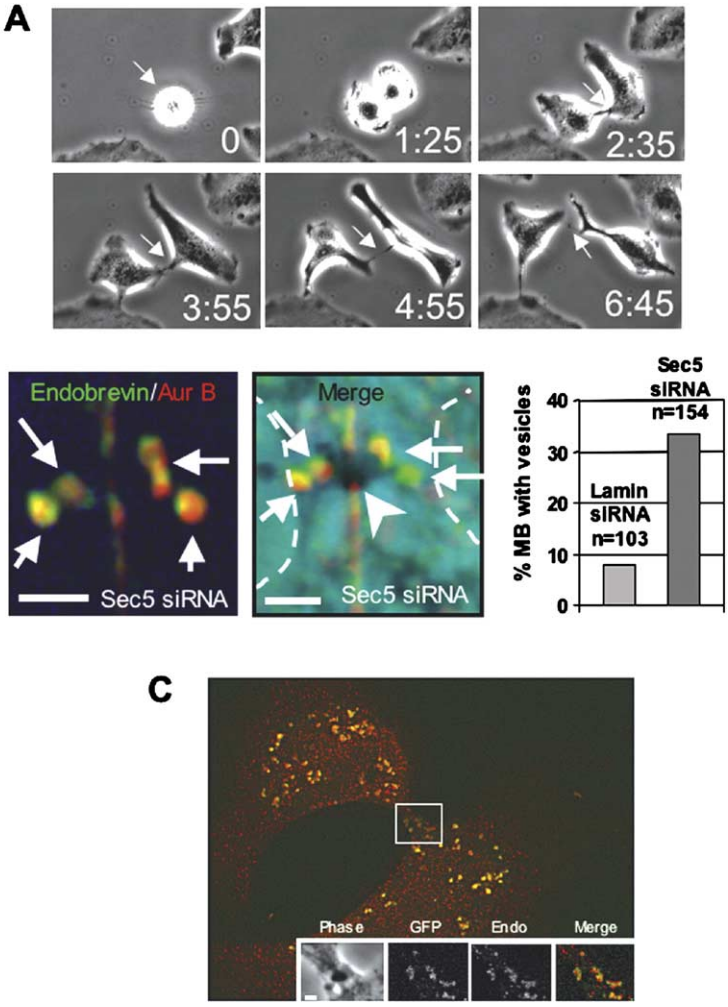

Figure 6. Disruption of the Exocyst Results in Accumulation of Secretory Vesicles at the Midbody Ring

(A) A mitotic cell (0, arrow) treated with BFA exits mitosis and forms a cleavage furrow with normal timing but arrests with a thin intercellular bridge that connects the two daughters (panels 2:35 through 6:45).

(B) sec5 siRNA-treated cells accumulate endobrevin/VAMP8-containing vesicle-like structures (arrows) at the Flemming body (arrowhead, panel 2). Dotted lines, plasma membrane. Graph, percentage of cells with endobrevin/VAMP8 vesicles at the midbody following indicated siRNA treatments. Scale bars, 2 μm.

(C) Endobrevin/VAMP8 (green) localizes to luminal-GFP secretory vesicles (red). Box at midbody is enlarged in insets. Endo, endobrevin/VAMP8.

tion of the exocyst, while localization of centriolin appears to be independent of the exocyst.

Disruption of the Exocyst Causes Failure at the Final Stages of Cytokinesis

Localization of the exocyst to the midbody and its interaction with centriolin suggested that the complex might play a role in cytokinesis. To examine this, we disrupted the midbody-associated exocyst using siRNAs targeting sec5 and examined cytokinesis by time-lapse imaging over a 20 hr time period. We found that over half the cells exhibited severe cytokinesis defects, including failure in the final abscission step (42%, Figures 4B and 4C, Movie S3) and delays during cytokinesis (24%, n = 18) compared with control lamin siRNA-treated cells (Figures 4A and 4C, Movie S2). Some cells remained interconnected by thin cytoplasmic bridges (Figure 4B, panel 17:05 and Movie S3) and sometimes entered one or more additional rounds of mitosis while still connected to their partner cells. Sec5-depleted cells viewed for an additional 24 hr showed a similar level of cytokinesis defects (data not shown), suggesting that nearly all cells in the culture experienced cytokinesis problems over time. Cytokinesis defects were also observed when the exocyst was disrupted by siRNA depletion of sec15 and sec8 (data not shown). Cells remained healthy, as no differences in cell morphology or mitochondrial function were observed. These data show that disruption of the exocyst produces late-stage cytokinesis defects similar to centriolin (Gromley et al., 2003) and demonstrates a requirement for the exocyst in the final stages of animal cell cytokinesis.

Snapin and SNARE Components Localize to the Midbody Ring in a Centriolin-Dependent Manner

Snapin was originally considered to be a neuron-specific protein, but recent studies demonstrated that it is also expressed in nonneuronal cells (Buxton et al., 2003). Snapin may facilitate assembly of SNARE complexes and may define a limiting step in vesicle fusion mediated by PKA phosphorylation (Chheda et al., 2001). Although the role of snapin in neurotransmission has been questioned (Vites et al., 2004), recent results indicate that it is essential for this process (Thakur et al., 2004). The role of snapin in cytokinesis is currently unknown. Using previously characterized antibodies to snapin (Thakur et al., 2004), we demonstrated that the

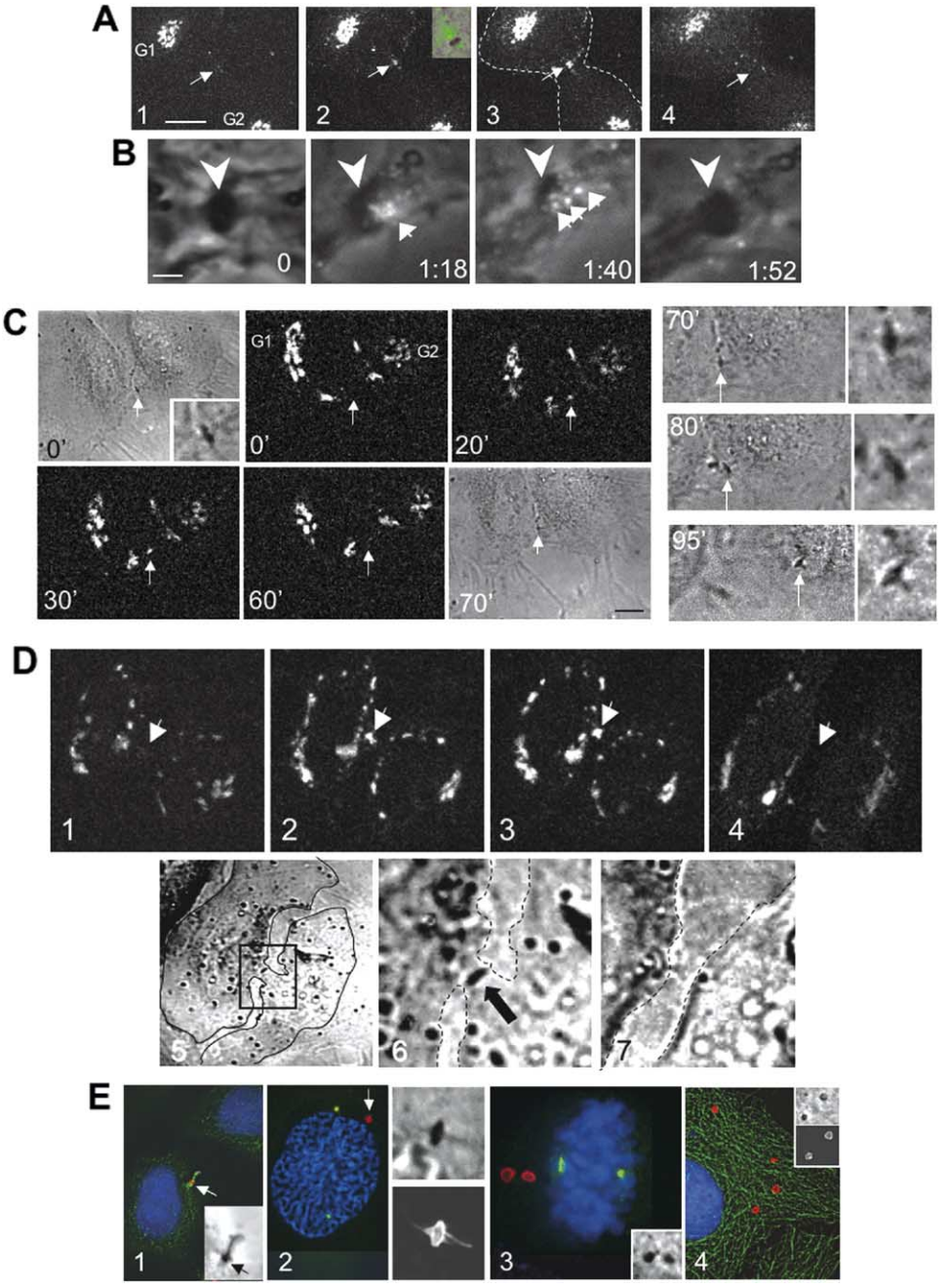

Figure 7. Asymmetric Delivery of Secretory Vesicles to One Side of the Flemming Body Is Followed by Abscission at This Site

(A) A dividing HeLa cell expressing luminal GFP accumulates secretory vesicles on one side of the Flemming body (arrows in 2 and 3, inset). In panel 1, most luminal-GFP signal is in Golgi complexes (G1 and G2). The signal appears transiently at one side of the midbody (2 and 3, arrows; Movie S5) and is lost, although Golgi signal remains (4). Scale bar in panel 1, 10 μm.

(B) Higher-magnification images of another cell (see Movie S6) showing unidirectional delivery of luminal-GFP-containing vesicles from one nascent daughter cell to one side of the Flemming body (arrowhead). GFP vesicles move to the Flemming body from the cell on the right (1:18 and 1:40, arrows; see Movie S6) and quickly disappear (1:52), presumably due to vesicle fusion with the plasma membrane and diffusion of the signal into the extracellular space. Phase and GFP signals are overlaid. Time, hr:min. Scale bar in panel 1, 1 μm.

(C) Lum-GFP vesicle delivery to the Flemming body (0'–30', arrows) followed by signal loss (60', at arrow) and abscission (80' and 95'). Phase-contrast images were taken after disappearance of GFP signal. Enlargements of Flemming body are shown to the right of each low-magnification image in 70'–95'. Scale bar at 70': 10 μm for 0'–95' and 2 μm for enlargements in 70'–95'.

(D) Lum-GFP vesicle delivery to one side of the midbody (panels 1–3) followed by disappearance of the GFP signal (panel 4) and abscission (loss of intercellular bridge, panels 5–7, arrows). The box in panel 5 is enlarged in panel 6. Solid and dotted lines show cell boundaries.

(E) Postmitotic cell (1) showing microtubules (green, GT335 antibody) of the intercellular bridge (phase-contrast image, inset) attached to one of the two daughter cells; no detectable midbody microtubules are seen on the other cell. Microtubules are on both sides of the midbody ring (arrow, red, MKLP-1) and Flemming body (inset, phase), showing that the midbody with attached microtubules was delivered to one daughter cell. Prophase HeLa cell (2) with condensing chromatin (blue) and two centrosomes (green) has a midbody ring and lateral material

protein localized to the midbody ring at the same time as the exocyst and shortly after centriolin (Figure 5A, panel 2).

Previous immunofluorescence studies showed that the v-SNARE endobrevin/VAMP8 and t-SNARE syntaxin-2 were enriched in the region of the midbody flanking the Flemming body and coincident with microtubules and Aurora B staining (Low et al., 2003). Using the same antibodies, we confirmed the localization pattern of endobrevin/VAMP8 (Figure 5A, panel 1) and syntaxin-2 (data not shown). Very late in cytokinesis, the intercellular bridge narrows to ~0.5 μm, and microtubule bundles are reduced in diameter to 0.2–0.5 μm. At this time, endobrevin/VAMP8 and syntaxin-2 joined centriolin, snapin, and the exocyst at the midbody ring (Figure 5A, panels 3 and 4). siRNA depletion of centriolin eliminated the midbody-ring localization of snapin (>35% of cells, Figure 5B), endobrevin/VAMP8 (>20% of cells, Figure 5C), and syntaxin-2 (Figure 5C). Of the remaining cells, 24% and 36% showed midbody staining levels below those of controls for snapin (n = 22) and endobrevin/VAMP8 (n = 25), respectively. As shown earlier, midbody-ring integrity was not compromised under these conditions, as MKLP-1 and MgcRacGAP remained at this site in cells with reduced centriolin. These results indicated that centriolin was required for midbody-ring localization of v- and t-SNARE proteins and the SNARE-associated protein snapin.

Snapin Depletion Mislocalizes the Protein from the Midbody and Induces Cytokinesis Defects

Midbodies in 41% of snapin-depleted cells showed no detectable snapin staining (Figure 5D). Time-lapse imaging over a 22 hr period showed that 40% of snapin-depleted cells experienced late-stage cytokinesis failure (Figure 5E, Movie S4). Other cells showed long delays and often remained connected by a thin intercellular bridge (data not shown). When cultures were imaged for an additional 24 hr, we observed multicellular syncytia resulting from multiple incomplete divisions and additional individual cells undergoing cytokinesis failure. This suggested that most cells in the population ultimately failed cytokinesis and that some failed multiple times. Occasionally, cells separated when one of the attached daughters re-entered mitosis, possibly due to tensile forces generated by cell rounding during mitosis (Figure 5E, Movie S4). These results demonstrated that snapin was necessary for abscission and suggested that it functioned by anchoring SNARE complexes at the midbody.

Disruption of the Exocyst Results in Accumulation of Secretory Vesicles at the Midbody

We next tested whether the late-stage cytokinesis defects observed in this study resulted from changes in membrane trafficking to the midbody. As a first test of this idea, we used brefeldin A, which disrupts cytokinesis in *C. elegans* presumably due to inhibition of post-Golgi secretory-vesicle trafficking (Skop et al., 2001). In HeLa cells treated with brefeldin A, we observed late-stage cytokinesis defects (Figure 6A) that were similar to those observed following depletion of centriolin. Many cells were delayed in or failed cytokinesis (n = 9/13 cells in two separate experiments). This suggested that post-Golgi vesicle trafficking was involved in late-stage cytokinesis events in vertebrate cells, although brefeldin A is known to affect other membrane-trafficking pathways (Antonin et al., 2000).

Based on the localization of the exocyst to the midbody ring, we reasoned that the vesicle-tethering function of the complex might be operating at this site to facilitate fusion of v-SNARE-containing vesicles at the late stages of cytokinesis. To test this idea, we depleted cells of sec5 to disrupt exocyst complexes and examined the localization of v-SNARE (endobrevin/VAMP8) containing vesicles. We observed a collection of small, spherical endobrevin/VAMP8-containing structures resembling vesicles at the midbody (Figure 6B, panel 1, arrows) that were positioned around the phase-dense Flemming body (Figure 6B, arrowhead, panel 2). Although these structures were occasionally seen in control lamin A/C siRNA-treated cells, they were significantly increased in sec5-depleted cells (Figure 6B, graph).

To determine whether the endobrevin/VAMP8-containing structures were secretory vesicles, we used a more specific marker for the secretory pathway. We expressed a GFP-tagged construct containing an amino-terminal signal peptide that targets the protein to the lumen of the ER (lum-GFP) (Blum et al., 2000) and lacks retention and retrieval motifs, so it would not be expected to target to endosomes, multivesicular bodies, or lysosomes. The lum-GFP was efficiently secreted from nondividing MDCK cells following a 19°C *trans*-Golgi network block and release from the block in the presence of protein-synthesis inhibitors (C.Y., unpublished data). When we expressed lum-GFP, numerous GFP-containing vesicles were observed in the cytoplasm. Following fixation and staining for endobrevin/VAMP8, we found that most of the endobrevin/VAMP8 vesicles colabeled with lum-GFP throughout the cytoplasm (Figure 6C) and within the intercellular bridge during late stages of cytokinesis (Figure 6C, insets). This observation demonstrates that the v-SNARE-containing vesicles that accumulated following disruption of the exocyst are secretory vesicles, an observation similar to that seen in studies in exocyst mutants of *S. cerevisiae* where vesicles dock normally but fail to fuse with the plasma membrane (Guo et al., 2000)

Asymmetric Delivery of Secretory Vesicles to the Midbody Is Followed by Abscission

At early stages of cytokinesis, we observed numerous GFP-labeled secretory vesicles in Golgi complexes and

stained with MKLP-1 (arrow, red) and in enlargement (bottom right); the Flemming body with flanking material is enlarged at upper right. Metaphase cell (3) with two midbody rings stained for MKLP-1 (red). Inset, two Flemming bodies corresponding to the two MKLP-1-stained structures. Centrosomes, green; DNA, blue. Interphase cell (4) showing four MKLP-1-stained midbody rings (red). Two are enlarged in lower inset and colocalize with phase-dense Flemming bodies (upper inset). DNA, blue; microtubules, green.

cell bodies of nascent daughter cells but few within intercellular bridges (Figure 7A, panel 1). However, at a late stage of cytokinesis when the intercellular bridge narrowed to a diameter of ~2 μm and the midbody microtubule bundle was reduced to a diameter of 0.5–1 μm, GFP secretory vesicles accumulated in the intercellular bridge near the midbody ring (Figure 7A, Movie S5). Higher-magnification imaging of another cell at a similar cell-cycle stage revealed labeled secretory vesicles moving suddenly and rapidly (within 20 min) from the cell bodies into the intercellular bridge and up to the midbody ring (Figure 7B, Movie S6). In 11/11 cells, the vesicles were delivered primarily if not exclusively from one of the nascent daughter cells (Figure 7B, center panels). Vesicles packed into the region adjacent to the phase-dense Flemming body (Figure 7B, panels 2 and 3, large arrowhead; Movie S6). Within 20 min, the GFP signal disappeared (Figure 7B, last panel and Figure 7A, last panel), suggesting that the vesicles fused with the plasma membrane, releasing the GFP signal into the extracellular space where it was free to diffuse. Loss of the GFP signal was not due to photobleaching because GFP-labeled vesicles in cell bodies adjacent to the intercellular bridge and in the Golgi complex retained the signal. We next examined the relationship between vesicle delivery to the midbody and abscission. We found that, shortly after the GFP signal was lost from the midbody region, the cell cleaved on the side of the Flemming body that received the GFP vesicles (6/6 cells from four experiments, Figure 7C). The cell on the opposite side received the Flemming body (Figure 7C, 70'–95' and Figure 7D). In some cases, the Flemming body moved around rapidly after abscission on the cell surface (Movie S7), suggesting that the structure was not anchored at a discrete point on the new daughter cell. Postdivision midbodies contained multiple midbody-ring components and retained microtubules from both sides of the midbody ring (Figure 7E, panel 1). They persisted for some time after abscission, consistent with previous results (Mishima et al., 2002), and were often present in multiple copies, suggesting that they were retained through several cell cycles (Figure 7E, panels 2–4). These structures were seen on ~35% of HeLa cells and often retained features of the Flemming body and midbody ring, including MKLP-1 staining, Aurora B staining, phase-dense Flemming bodies, and localization to the plasma membrane (Figure 7E, data not shown). This suggested that supernumerary midbodies represent structures from previous divisions similar to the bud scars observed in yeast (Chen and Contreras, 2004).

Discussion

A Model for the Final Stage of Cytokinesis

This study defines several distinct molecular and structural steps during the late stages of cytokinesis (Figure 8). During cleavage-furrow ingression, MKLP-1 and MgcRacGAP arrive at the midbody ring (Figure 8A). When the intercellular bridge forms, centriolin localizes to the ring (Figure 8B), followed by snapin and exocyst proteins (Figure 8C). When the diameter of the midbody microtubule bundle and the intercellular bridge are reduced to ~0.5–1 μm, endobrevin/VAMP8 (v-SNARE) and syntaxin-2 (t-SNARE) move to the midbody ring. The v-SNAREs are part of secretory vesicles that move asymmetrically into the intercellular bridge predominantly from one nascent daughter cell; binding to v-SNAREs may incorporate t-SNAREs into this organization. The vesicles pack into the area adjacent to the ring and appear to fuse, releasing their contents into the extracellular space (lum-GFP, Figures 8D and 8E). Vesicle fusion with the plasma membrane may be initiated near the midbody ring where v- and t-SNAREs are localized. This could be followed by additional fusion events between vesicles and the plasma membrane as well as vesicle-vesicle fusion events (homotypic) mediated by SNAP23/25, a v-SNARE involved in compound exocytosis (Takahashi et al., 2004) (Figures 8F and 8G). Abscission then occurs at the site of vesicle fusion, and the entire midbody remains with the daughter cell opposite the fusion site (Figure 8H). Abscission could be triggered by arrival of v- and t-SNAREs at the midbody ring; release of SNAP23/25 from lipid rafts (Takahashi et al., 2004; Takeda et al., 2004); phosphorylation of snapin by PKA, which mediates its binding to the t-SNARE complex (Buxton et al., 2003; Chheda et al., 2001); or another event. Dynamic movement of the postabscission midbody ring suggests connections to motile forces within the cell, although this remains to be determined.

Asymmetric Delivery of Secretory Vesicles Marks the Site of Abscission

It is remarkable that secretory vesicles loaded with luminal GFP move into the intercellular bridge from only one of the two prospective daughter cells. The mechanism of this asymmetric vesicle delivery is unknown. It is tempting to speculate that a signal, negative or positive, emanates asymmetrically from one centrosome in the dividing cell. Centrosomes in the two prospective daughter cells are different in that one was "born" from the older centriole in the previous cell division during the centrosome duplication process (Doxsey, 2001). Consistent with this idea is the asymmetric spindle-pole body (SPB) localization of budding- and fission-yeast proteins that control mitotic exit and cytokinesis (Doxsey et al., 2005; Grallert et al., 2004; Molk et al., 2004). In *S. pombe*, inhibitors of mitotic exit (Cdc16p and Byr4p) localize to the "old" SPB while activators of mitotic exit (Cdc7p and presumably Sid1p and Cdc14p) localize to the new SPB (Grallert et al., 2004). The relevance of this localization in both yeasts is still unknown. Further studies will be required to determine the role of centrosome protein asymmetry in the unidirectional delivery of secretory vesicles and abscission in animal cells. It has been suggested that the mother centriole moves to the intercellular bridge in telophase cells to coordinate the final steps in cytokinesis (Piel et al., 2001), although this was not consistently observed in this study (data not shown) or another that investigated several cell lines (RPE-1, Ptk-1, CV-1, NRK-52E; A. Khodjakov, personal communication).

The final stages of cytokinesis in animal cells share features with cell division in higher plants. Higher plant cells cannot divide using an actomyosin-based cleavage furrow due to the presence of a nonpliant cell wall,

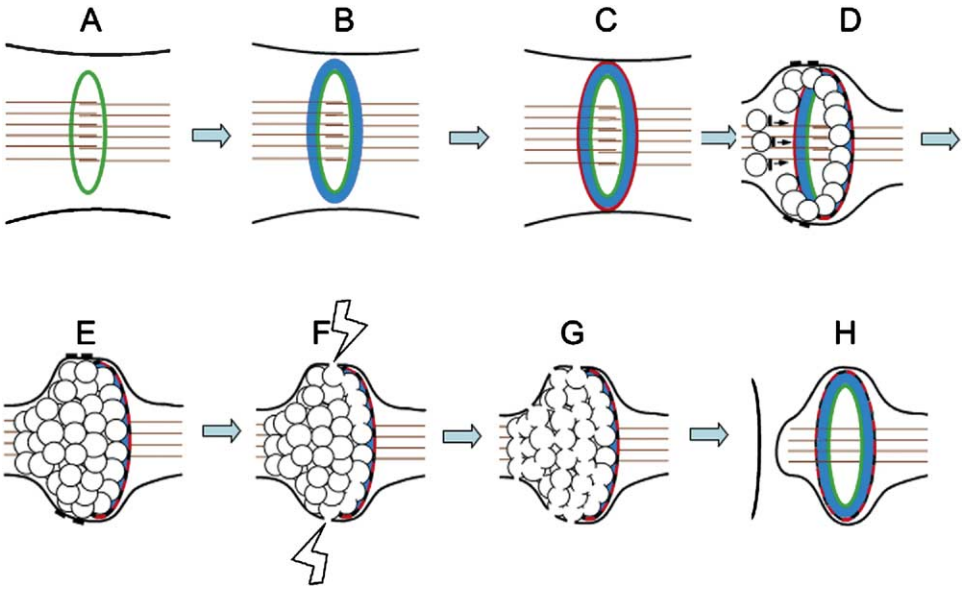

Figure 8. Model Depicting Vesicle-Mediated Abscission during Cytokinesis

(See text for details.)

(A) MKLP-1 and MgcRacGAP (green) arrive at midbody ring after cleavage furrowing has progressed. Microtubules, brown; plasma membrane, upper and lower lines.

(B and C) Centriolin moves to ring ([B], blue) and anchors sec15, other exocyst components, and snapin ([C], red).

(D) When midbody microtubules are reduced and the membrane constricted, v- and t-SNAREs ([D], black) move to the midbody ring from one prospective daughter cell. v-SNAREs presumably move with vesicles and bind there in a centriolin-dependent manner; t-SNAREs on the plasma membrane could bind through v-SNAREs.

(E) Vesicles heterogeneous in diameter pack asymmetrically into the intercellular bridge adjacent to the midbody ring.

(F and G) Vesicles adjacent to the ring containing SNARES and exocyst fuse with the plasma membrane (F) as well as at other plasma-membrane sites and with one another (G).

(H) Abscission follows at the site of membrane fusion, and the midbody is retained by the daughter cell opposite the fusion site. The released midbody ring contains multiple midbody-ring proteins and usually retains microtubule bundles from both sides of the ring. (In this model, the apparent "layering" of components is a simplification to depict arrival of different components at the midbody.)

so they accomplish cell division by constructing a new membrane at the division plane, called the cell plate, that is independent of the plasma membrane and is established by microtubule-dependent delivery and fusion of vesicles at this site (Albertson et al., 2005; Finger and White, 2002; Jurgens, 2005). Our data show that the coordinated delivery of vesicles to the midbody ring during the late stages of cytokinesis is also required for the final stages of cell division in animal cells. However, we still do not understand the mechanism of secretory-vesicle delivery to the midbody, the role of microtubules in this process, or the precise contribution of vesicle transport and fusion to abscission. The presence of vesicles with heterogeneous diameters adjacent to the midbody ring prior to abscission is consistent with a model in which some vesicles fuse together prior to fusion with the plasma membrane. This would be analogous to the cell plate in plant cells. The enodocytic pathway also appears to play a role in cell cleavage as components (dynamin, FIP3, Rab11) and compartments (endosomes) involved in this pathway affect the late stages of cytokinesis (Thompson et al., 2002; Wilson et al., 2005). Recycling endosomes have been shown to move from both prospective daughter cells to the midbody during cytokinesis then return to the daughter-cell cytoplasm (Wilson et al., 2005). It is still unclear how recycling endosomes participate in abscission and how the bidirectional movement of endosomes into the intercellular bridge is related to the unidirectional movement of secretory vesicles to this site in our study.

Structure and Persistence of the Midbody Ring

We have shown that many proteins localize to the midbody ring and that the phase-dense Flemming body is also organized into the shape of a ring. This is consistent with earlier ultrastructural studies that describe cytoplasmic channels coursing through the central midbody (Mullins and Biesele, 1977). The ring structure bears a resemblance to bud scars of *S. cerevisiae,* which serve as markers for longevity (Chen and Contreras, 2004). The midbody ring in animal cells is inherited by the daughter cell that lies opposite the site of vesicle delivery and appears to persist, as it is often seen in mitotic cells prior to cytokinesis and found in multiple copies in interphase cells (Figure 7E) (Mishima et al., 2002). Shortly after abscission, the midbody ring contains microtubules that extend from both sides of the ring. This suggests that dissolution of microtubule bundles adjacent to the midbody ring is not an absolute requirement for the final stage of cytokinesis but rather that abscission can result in transfer of the entire mid-

body and associated microtubules into one daughter cell.

Experimental Procedures

Cell Culture and Transfections

The cells used primarily in this study were diploid, telomerase-immortalized human RPE cells (hTERT-RPE-1s, Clontech Laboratories, Inc.) (Morales et al., 1999) and HeLa cells. All cells were grown as previously described (American Type Culture Collection). HeLa cells were transfected as previously described (Lipofectamine, Invitrogen).

Immunofluorescence

Cells were prepared for immunofluorescence, imaged, and deconvolved (Metamorph, Universal Imaging Corp.) using either formaldehyde, formaldehyde followed by methanol, or methanol alone as previously described (Dictenberg et al., 1998). All immunofluorescence images are two-dimensional projections of three-dimensional reconstructions to ensure that all stained material was visible in two-dimensional images. Quantification of signals produced by immunofluorescence staining for various midbody antigens was performed as described for centrosome protein quantification in our earlier studies (Gromley et al., 2003).

Antibodies

Antibodies to the following proteins were used: sec3, sec5, sec8, sec10, exo70, exo84, and sec15 (Yeaman, 2003); centriolin (Gromley et al., 2003); α-tubulin, γ-tubulin, α-His_6, and α-myc (Sigma-Aldrich); Aurora B (Transduction Laboratories); MKLP-1, GAL4 transactivation domain (AD), and GAL4 DNA binding domain (DBD) (Santa Cruz Biotechnology, Inc.); and GT335 for stabilized microtubules (Gromley et al., 2003).

Yeast Two-Hybrid Screen

Yeast two-hybrid library screens were performed following the manufacturer's instructions using a human testis Matchmaker Pre-Transformed Two-Hybrid Library (Matchmaker GAL4 Yeast Two-Hybrid System, Clontech). False positives were eliminated by mating each clone with strains expressing either lamin C or the DNA binding domain alone and plating on quadruple dropout media.

siRNAs

Two siRNAs targeting centriolin and one targeting lamin A/C were used as described (Gromley et al., 2003). Additional siRNAs targeted nucleotides in the following proteins: MKLP-1 (189–207), sec5 (260–278), sec8 (609–627), and snapin (312–330). Cells were examined 24–48 hr after siRNA treatment. siRNAs were used at 10–50 nM, and Lipofectamine was the delivery agent (Gromley et al., 2003).

Brefeldin A Treatment

HeLa cells were treated with 5–10 μg/ml brefeldin A (Sigma-Aldrich) and imaged.

Immunoprecipitations

Antibodies to centriolin or exocyst were added to hTERT-RPE cell extracts and incubated at 4°C overnight. The lysis buffer included 50 mM Tris-HCl (pH 7.5), 10 mM Na_2HPO_4 (pH 7.2), 1 mM EDTA, 150 mM NaCl, 1% IGEPAL CA-1630, and protease inhibitors (Mini tablets, Roche Diagnostics, Mannheim, Germany). Superose 6 samples were incubated with antibodies to sec3 and sec8, bound to protein A/G beads (Santa Cruz Biotechnology, Inc.) at 4°C for 2 hr (Yeaman, 2003), and exposed to SDS-PAGE and immunoblotting (Harlow and Lane, 1988).

Time-Lapse Imaging

Time-lapse imaging of cytokinesis was performed using a wide-field microscope (Gromley et al., 2003), and images were taken every 5 min for 18–24 hr. For luminal-GFP-expressing cells (Figure 7B), two concurrent time-lapse programs were used (GFP, phase contrast), and images were taken every 2 min for 3–4 hr. A PerkinElmer spinning-disc confocal microscope with an UltraVIEW CSU-10 head was used for Figures 7A, 7C, and 7D. Images were taken every 5 min and captured on an ORCA-AG cooled CCD camera. Images of GFP-GAPCenA-expressing cells were taken every 10 min on a Zeiss Axiophot microscope equipped with a Hamamatsu digital camera. Mitochondria function was assessed by Mitotracker staining (Molecular Probes).

Exocyst Fractionation

For isopycnic centrifugation, membrane compartments containing exocyst fractions were prepared as described (Grindstaff et al., 1998; Yeaman, 2003). For size-exclusion chromatography, cells were extracted with MEBC buffer (0.5% Nonidet P-40, 50 mM Tris-HCl [pH 7.5], 100 mM NaCl) containing protease inhibitors (0.1 mM Na_3VO_4; 50 mM NaF; 1 mM Pefabloc [Boehringer Mannheim]; and 10 μg/ml each of leupeptin, antipain, chymostatin, and pepstatin A) for 10 min at 4°C. Lysates were first sedimented in a Microfuge (Beckman Instruments, Fullerton, California) for 10 min and then for 30 min at 100,000 × g, passed through a 0.22 μm filter (Millipore), and loaded on a Superose 6 HR 10/30 column (200 μl, 10 mm × 30 cm; Pharmacia Biotech, Inc.) equilibrated in MEBC buffer and 1 mM dithiothreitol with 0.1 mM Pefabloc. Proteins were eluted (0.3 ml/min) at 17°C in 0.5 ml fractions, the concentration of protein in the fractions was determined, and the fractions were used for various assays (fractions 7–30).

Supplemental Data

Supplemental Data include one figure and seven movies and can be found with this article online at http://www.cell.com/cgi/content/full/123/1/75/DC1/.

Acknowledgments

We thank Dan McCollum, Yu-Li Wang, Ted Salmon, and Bill Theurkauf for useful discussions. We thank Z. Sheng (NINDS, NIH) (snapin), T. Wiembs (Lerner Institute, Cleveland) (endobrevin/VAMP8 and syntaxin-2) and M. Glotzer (IMP, Vienna) (MKLP-1, MgcRacGAP) for antibodies. This work was supported in part by grants from the National Institutes of Health to S.J.D. (GM51994) and from the Department of Defense to C.Y. (DAMD-17-03-1-0187).

Received: August 18, 2004
Revised: June 3, 2005
Accepted: July 27, 2005
Published: October 6, 2005

References

Albertson, R., Riggs, B., and Sullivan, W. (2005). Membrane traffic: a driving force in cytokinesis. Trends Cell Biol. *15*, 92–101.

Antonin, W., Holroyd, C., Tikkanen, R., Honing, S., and Jahn, R. (2000). The R-SNARE endobrevin/VAMP-8 mediates homotypic fusion of early endosomes and late endosomes. Mol. Biol. Cell *11*, 3289–3298.

Blum, R., Stephens, D.J., and Schulz, I. (2000). Lumenal targeted GFP, used as a marker of soluble cargo, visualises rapid ERGIC to Golgi traffic by a tubulo-vesicular network. J. Cell Sci. *113*, 3151–3159.

Buxton, P., Zhang, X.M., Walsh, B., Sriratana, A., Schenberg, I., Manickam, E., and Rowe, T. (2003). Identification and characterization of Snapin as a ubiquitously expressed SNARE-binding protein that interacts with SNAP23 in non-neuronal cells. Biochem. J. *375*, 433–440.

Chen, C., and Contreras, R. (2004). The bud scar-based screening system for hunting human genes extending life span. Ann. N Y Acad. Sci. *1019*, 355–359.

Chheda, M.G., Ashery, U., Thakur, P., Rettig, J., and Sheng, Z.H. (2001). Phosphorylation of Snapin by PKA modulates its interaction with the SNARE complex. Nat. Cell Biol. *3*, 331–338.

Cuif, M.H., Possmayer, F., Zander, H., Bordes, N., Jollivet, F., Couedel-Courteille, A., Janoueix-Lerosey, I., Langsley, G., Bornens, M., and Goud, B. (1999). Characterization of GAPCenA, a GTPase

activating protein for Rab6, part of which associates with the centrosome. EMBO J. *18*, 1772–1782.

Dictenberg, J., Zimmerman, W., Sparks, C., Young, A., Vidair, C., Zheng, Y., Carrington, W., Fay, F., and Doxsey, S.J. (1998). Pericentrin and gamma tubulin form a protein complex and are organized into a novel lattice at the centrosome. J. Cell Biol. *141*, 163–174.

Dobbelaere, J., and Barral, Y. (2004). Spatial coordination of cytokinetic events by compartmentalization of the cell cortex. Science *305*, 393–396.

Doxsey, S. (2001). Re-evaluating centrosome function. Nat. Rev. Mol. Cell Biol. *2*, 688–698.

Doxsey, S., McCollum, D., and Theurkauf, W. (2005). Centrosomes in cellular regulation. Annu. Rev. Cell Dev. Biol. *21*, 688–698. in press.

Echard, A., Hickson, G.R., Foley, E., and O'Farrell, P.H. (2004). Terminal cytokinesis events uncovered after an RNAi screen. Curr. Biol. *14*, 1685–1693.

Finger, F.P., and White, J.G. (2002). Fusion and fission: membrane trafficking in animal cytokinesis. Cell *108*, 727–730.

Finger, F.P., Hughes, T.E., and Novick, P. (1998). Sec3p is a spatial landmark for polarized secretion in budding yeast. Cell *92*, 559–571.

Glotzer, M. (2001). Animal cell cytokinesis. Annu. Rev. Cell Dev. Biol. *17*, 351–386.

Glotzer, M. (2005). The molecular requirements for cytokinesis. Science *307*, 1735–1739.

Grallert, A., Krapp, A., Bagley, S., Simanis, V., and Hagan, I.M. (2004). Recruitment of NIMA kinase shows that maturation of the S. pombe spindle-pole body occurs over consecutive cell cycles and reveals a role for NIMA in modulating SIN activity. Genes Dev. *18*, 1007–1021.

Grindstaff, K.K., Yeaman, C., Anandasabapathy, N., Hsu, S.C., Rodriguez-Boulan, E., Scheller, R.H., and Nelson, W.J. (1998). Sec6/8 complex is recruited to cell-cell contacts and specifies transport vesicle delivery to the basal-lateral membrane in epithelial cells. Cell *93*, 731–740.

Gromley, A., Jurczyk, A., Sillibourne, J., Halilovic, E., Mogensen, M., Groisman, I., Blomberg, M., and Doxsey, S. (2003). A novel human protein of the maternal centriole is required for the final stages of cytokinesis and entry into S phase. J. Cell Biol. *161*, 535–545.

Guertin, D.A., Trautmann, S., and McCollum, D. (2002). Cytokinesis in eukaryotes. Microbiol. Mol. Biol. Rev. *66*, 155–178.

Guo, W., Sacher, M., Barrowman, J., Ferro-Novick, S., and Novick, P. (2000). Protein complexes in transport vesicle targeting. Trends Cell Biol. *10*, 251–255.

Harlow, E., and Lane, D. (1988). Antibodies: A Laboratory Manual (Cold Spring Harbor, NY: Cold Spring Harbor Laboratory Press).

Jurgens, G. (2005). Plant cytokinesis: fission by fusion. Trends Cell Biol. *15*, 277–283.

Low, S.H., Li, X., Miura, M., Kudo, N., Quinones, B., and Weimbs, T. (2003). Syntaxin 2 and endobrevin are required for the terminal step of cytokinesis in mammalian cells. Dev. Cell *4*, 753–759.

Mishima, M., Kaitna, S., and Glotzer, M. (2002). Central spindle assembly and cytokinesis require a kinesin-like protein/RhoGAP complex with microtubule bundling activity. Dev. Cell *2*, 41–54.

Molk, J.N., Schuyler, S.C., Liu, J.Y., Evans, J.G., Salmon, E.D., Pellman, D., and Bloom, K. (2004). The differential roles of budding yeast Tem1p, Cdc15p, and Bub2p protein dynamics in mitotic exit. Mol. Biol. Cell *15*, 1519–1532.

Mondesert, G., Clarke, D.J., and Reed, S.I. (1997). Identification of genes controlling growth polarity in the budding yeast Saccharomyces cerevisiae: a possible role of N-glycosylation and involvement of the exocyst complex. Genetics *147*, 421–434.

Monzo, P., Gauthier, N.C., Keslair, F., Loubat, A., Field, C.M., Le Marchand-Brustel, Y., and Cormont, M. (2005). Clues to CD2-associated protein involvement in cytokinesis. Mol. Biol. Cell *16*, 2891–2902. 10.1091/mbc.E04-09-0773

Morales, C.P., Holt, S.E., Ouellette, M., Kaur, K.J., Yan, Y., Wilson, K.S., White, M.A., Wright, W.E., and Shay, J.W. (1999). Absence of cancer-associated changes in human fibroblasts immortalized with telomerase. Nat. Genet. *21*, 115–118.

Mullins, J.M., and Biesele, J.J. (1977). Terminal phase of cytokinesis in D-98s cells. J. Cell Biol. *73*, 672–684.

Murthy, M., and Schwarz, T.L. (2004). The exocyst component Sec5 is required for membrane traffic and polarity in the Drosophila ovary. Development *131*, 377–388.

Papoulas, O., Hays, T.S., and Sisson, J.C. (2004). The golgin Lava lamp mediates dynein-based Golgi movements during Drosophila cellularization. Nat. Cell Biol. *7*, 612–618. 10.1038/ncb1264

Paweletz, N. (1967). On the function of the 'Flemming body' during division of animal cells. Naturwissenschaften *54*, 533–535.

Piel, M., Nordberg, J., Euteneuer, U., and Bornens, M. (2001). Centrosome-dependent exit of cytokinesis in animal cells. Science *291*, 1550–1553.

Prigent, M., Dubois, T., Raposo, G., Derrien, V., Tenza, D., Rosse, C., Camonis, J., and Chavrier, P. (2003). ARF6 controls post-endocytic recycling through its downstream exocyst complex effector. J. Cell Biol. *163*, 1111–1121.

Salminen, A., and Novick, P.J. (1989). The Sec15 protein responds to the function of the GTP binding protein, Sec4, to control vesicular traffic in yeast. J. Cell Biol. *109*, 1023–1036.

Saxton, W.M., and McIntosh, J.R. (1987). Interzone microtubule behavior in late anaphase and telophase spindles. J. Cell Biol. *105*, 875–886.

Skop, A.R., Bergmann, D., Mohler, W.A., and White, J.G. (2001). Completion of cytokinesis in C. elegans requires a brefeldin A-sensitive membrane accumulation at the cleavage furrow apex. Curr. Biol. *11*, 735–746.

Skop, A.R., Liu, H., Yates, J., Meyer, B.J., and Heald, R. (2004). Dissection of the mammalian midbody proteome reveals conserved cytokinesis mechanisms. Science *305*, 61–66. Published online May 27, 2004..

Strickland, L.I., and Burgess, D.R. (2004). Pathways for membrane trafficking during cytokinesis. Trends Cell Biol. *14*, 115–118.

Takahashi, N., Hatakeyama, H., Okado, H., Miwa, A., Kishimoto, T., Kojima, T., Abe, T., and Kasai, H. (2004). Sequential exocytosis of insulin granules is associated with redistribution of SNAP25. J. Cell Biol. *165*, 255–262.

Takeda, T., Kawate, T., and Chang, F. (2004). Organization of a sterol-rich membrane domain by cdc15p during cytokinesis in fission yeast. Nat. Cell Biol. *6*, 1142–1144.

Thakur, P., Stevens, D.R., Sheng, Z.H., and Rettig, J. (2004). Effects of PKA-mediated phosphorylation of Snapin on synaptic transmission in cultured hippocampal neurons. J. Neurosci. *24*, 6476–6481.

Thompson, H.M., Skop, A.R., Euteneuer, U., Meyer, B.J., and McNiven, M.A. (2002). The large GTPase dynamin associates with the spindle midzone and is required for cytokinesis. Curr. Biol. *12*, 2111–2117.

Verplank, L., and Li, R. (2005). Cell cycle-regulated trafficking of Chs2 controls actomyosin ring stability during cytokinesis. Mol. Biol. Cell *16*, 2529–2543.

Vites, O., Rhee, J.S., Schwarz, M., Rosenmund, C., and Jahn, R. (2004). Reinvestigation of the role of snapin in neurotransmitter release. J. Biol. Chem. *279*, 26251–26256.

Wang, H., Tang, X., Liu, J., Trautmann, S., Balasundaram, D., McCollum, D., and Balasubramanian, M.K. (2002). The multiprotein exocyst complex is essential for cell separation in Schizosaccharomyces pombe. Mol. Biol. Cell *13*, 515–529.

Wilson, G.M., Fielding, A.B., Simon, G.C., Yu, X., Andrews, P.D., Hames, R.S., Frey, A.M., Peden, A.A., Gould, G.W., and Prekeris, R. (2005). The FIP3-Rab11 protein complex regulates recycling endosome targeting to the cleavage furrow during late cytokinesis. Mol. Biol. Cell *16*, 849–860.

Yeaman, C. (2003). Ultracentrifugation-based approaches to study regulation of Sec6/8 (exocyst) complex function during development of epithelial cell polarity. Methods *30*, 198–206.

Yeaman, C., Grindstaff, K.K., and Nelson, W.J. (2004). Mechanism of recruiting Sec6/8 (exocyst) complex to the apical junctional complex during polarization of epithelial cells. J. Cell Sci. *117*, 559–570.